

Investigating the Spatiotemporal Charging Demand and Travel Behavior of Electric Vehicles Using GPS Data: A Machine Learning Approach

Sina Baghali, *Graduate Student Member, IEEE*, Zhaomiao Guo, Samiul Hasan

Civil, Environmental, and Construction Engineering, University of Central Florida, Orlando, FL, USA

baghalisina@knights.ucf.edu, guo@ucf.edu, samiul.hasan@ucf.edu

Abstract—The increasing market penetration of electric vehicles (EVs) may change the travel behavior of drivers and pose a significant electricity demand on the power system. Since the electricity demand depends on the travel behavior of EVs, which are inherently uncertain, the forecasting of daily charging demand (CD) will be a challenging task. In this paper, we use the recorded GPS data of EVs and conventional gasoline-powered vehicles from the same city to investigate the potential shift in the travel behavior of drivers from conventional vehicles to EVs and forecast the spatiotemporal patterns of daily CD. Our analysis reveals that the travel behavior of EVs and conventional vehicles are similar. Also, the forecasting results indicate that the developed models can generate accurate spatiotemporal patterns of the daily CD.

Index Terms—Electric vehicles, charging demand, travel behavior, GPS data, machine learning

I. INTRODUCTION

The transportation sector is the second-largest source of greenhouse gas emissions (GHGs) [1]. Electric vehicles (EVs), receiving increased popularity, provide an effective way to control GHGs and fossil fuel consumption. With EVs passing 10 million counts in 2020 worldwide [2], it is foreseeable that EVs will comprise a significant market share of the future transportation fleet, which may cause shifts in travel behavior in the transportation systems and influence the power system operation. According to the International Energy Agency (IEA), the EV fleet will impose 860 TWh of electricity demand by 2030 [2]. Therefore, the spatial and temporal behavior of EV charging demand (CD) is vital for power system planning and operation.

The literature in modeling EV CD can be discussed from two aspects: 1) the input data used; and 2) the applied modeling methodologies. Survey data are the classic sources of data used in multiple studies for modeling the driving and charging behavior of EVs [3]–[5]. However, survey data may be costly to collect and can only provide a perceived travel behavior. Mobile phone and social network data with location tags may not be an appropriate source for analyzing the behavior of EVs because the mode of transportation can not be accurately estimated. Among the mobility data sources, GPS data is the best fit to model and estimate the actual behavior of EVs. With high-resolution location tracking, we can record the driving distance of each trip, calculate the resulting CD of the vehicles, and estimate locations where charging stations are mostly needed. Additionally, the high sample frequency of GPS data can help model the temporal behaviors of EVs accurately. In earlier studies [6], [7], the GPS data of conventional

internal combustion engine vehicles (ICEVs) were considered as EVs and derived charging behaviors based on their travel behaviors. Current studies also use the GPS data of ICEVs to infer the feasibility and potentials of electrifying the existing transportation fleet [8], [9]. These data sources, however, can not account for the behavior of EVs since they are either small-scale data of limited ICEVs or GPS data of specific vehicle types, e.g., taxi fleet [6], [8], [9].

After selecting one of the data sources discussed, studies implement different methodologies to model and estimate the charging and travel behavior of EVs. Stochastic modeling is the most popular method applied in many studies for investigating the stochastic behavior of CD [4], [10]–[13]. Stochastic modeling considered in the studies are either based on Monte-Carlo Simulation (MCS) [12] or Markov chain modeling [13]. Both cases of stochastic modeling require many scenario generations, which is computationally expensive, and they neglect the correlation of travel parameters.

Machine learning algorithms, such as k-nearest neighbors (KNN) [4] or artificial neural networks [3], [14], [15], are recently adopted in CD estimation. However, studies in [14], [15] incorporate probabilistic models to generate synthetic trips to overcome the small scale of their input data. In [3], a large survey data is used for estimating the travel parameters and CD. However, the authors assume smart charging of EV users where a centralized entity determines the optimal time for charging and shifts the charging time to the hours with low charging price, which may not represent the realistic daily CD.

In this study, we seek to resolve the aforementioned drawbacks by using GPS data for EVs and developing machine learning models to estimate the daily CD. Unlike [8], [9] that considered GPS data of ICEVs as EVs, we have examined the data of actual EVs and provided extensive comparison on the traveling behavior of EVs and ICEVs commuting in the same urban network. Additionally, we have analyzed the CD of EVs based on their recorded state of charge (SOC) without making assumptions on EVs' initial SOC and energy consumption based on the traveling distances, which is a prevalent assumption made in different studies due to the lack of information in the data sets [3], [5], [15]. Lastly, different from studies like [3], [14], [15] that have focused on temporal behavior of the CD, we have developed forecasting models to extract and estimate both the spatial and temporal behavior of CD.

TABLE I
INPUT DATA EXAMPLE

Day No.	Vehicle ID	Trip No.	Time stamp (ms)	Latitude (deg)	Longitude (deg)	SOC (%)
5.5602	371	1288	0	42.2776	-83.7537	94.344
5.5602	371	1288	600	42.2776	-83.7537	94.344
5.5602	371	1288	700	42.2776	-83.7537	94.344
5.5602	371	1288	1700	42.2776	-83.7537	94.344

II. DATA DESCRIPTION

We will use vehicle energy dataset (VED) ¹, which is a publicly available data set containing GPS trajectories of a limited number of personal cars including both ICEVs and EVs in Ann Arbor, Michigan, the USA from Nov 2017 to Nov 2018 [16]. This is a unique data set providing high-resolution data of EVs' energy consumption and their state of charge (SOC). The VED contains trajectories of 383 vehicles, including 264 ICEVs, 92 hybrid EVs (HEVs), and 27 plug-in HEV (PHEVs/EVs). The VED consists of dynamic and static data sets; Static data contains vehicle parameters (e.g., vehicle ID, vehicle type, vehicle class, etc.), and dynamic data contains high-resolution daily trip trajectories and other trip parameters (e.g., day number, trip number, latitude, location latitude, and longitude, etc.). We will derive the vehicle IDs of EVs from static data and use them to extract the dynamic data of EVs based on vehicle ID. The collected dynamic data has different features of the trips. Among them, we will use day number, vehicle ID, trip number, timestamps (ms), latitude, longitude, and state of charge (SOC) of batteries. Table I shows a sample of the input data with the selected features for an EV as an example.

We can calculate the trip duration and end time by considering the last timestamp recorded for each trip. Trip distance is another important parameter that can be extracted with the recorded latitudes and longitudes at each timestamp by calculating the distance between each consecutively recorded timestamp and aggregating over the records of each trip using the Haversian formula [17]. The other key feature of the input data is the recorded SOC of batteries in each timestamp. Therefore, we don't need to make assumptions about the initial SOC of EVs and calculate the consumed energy based on trip distance. With the recorded SOC values, we can determine the consumed energy in trips and calculate the CD.

After applying all the data preprocessing procedures discussed above, we can derive the parameters of each trip, i.e., trip start time, end time, origin and destination (OD) locations, and consumed energy.

III. TRAVEL BEHAVIOR COMPARISON

The processed input data contains the records of 4,109 trips made by EVs during one year. This data can be used to extract the distribution of trip parameters, e.g., trip distance, trip start and end time, number of daily trips, etc., and presents an opportunity to compare the behavior of EVs and conventional ICEVs. Therefore, we repeated the same initial data processing on the dynamic trip data of ICEVs, and the result was the

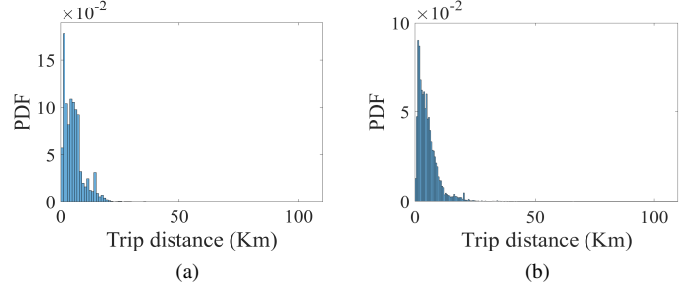


Fig. 1. Distribution of daily trips (a) EVs (b) ICEVs

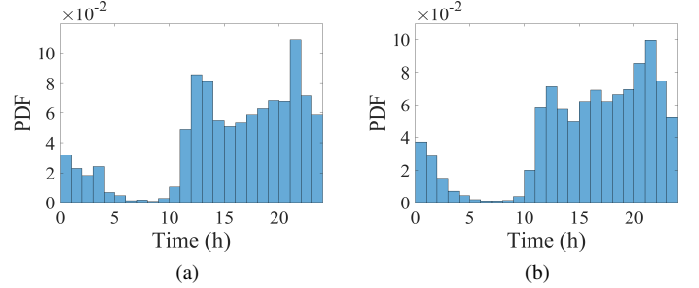


Fig. 2. Distribution of daily trips' start time (a) EVs (b) ICEVs

records of 18,936 trips made by ICEVs. We will use both of these data sets to compare the travel behavior between ICEVs and EVs.

Fig. 1 shows the distribution of daily trip distances for both EVs (Fig. 1a) and ICEVs (Fig. 1b). The short distance trips (0~20 Km) are more prevalent in both types of vehicles, and the main difference is the maximum trip distance. ICEVs have a higher maximum trip distance (110 Km), where the maximum trip distance recorded for EVs is 35 Km. One can infer that ICEVs are preferred for long-distance trips. However, since the frequency of such trips is low, no general trends can be derived.

The trips' start and end time distributions are shown in Fig. 2 and 3 for both types of vehicles. There are no major differences between the trip start time distributions for EVs and ICEVs (see Fig. 2). Minor difference can be seen in the trip end time of EVs compared to ICEVs. EVs tend to finish their trips less during $t = 23 \sim 1$ (see Fig. 3a), whereas more trip end time has been recorded for ICEVs during that time (see Fig. 3b). Also, trip end time during $t = 10 \sim 15$ has been more prevalent among EVs compared to ICEVs. This might be because of the charging needs of EVs after the trips or user preference of the drivers.

In summary, EVs and ICEVs have similar patterns on trip start/end time and distance per trip. But ICEVs owners may be more likely to have more daily trips and ICEVs are preferred for trips with long distances. Also, EVs tend to end their trip more during the afternoons and less close to the midnight.

IV. CHARGING DEMAND MODELING

In this section, we will derive the daily spatiotemporal CD behavior based on the input data. In order to detect the charging events, we will compare the SOC of the EVs at the

¹Data: <https://github.com/gsoh/VED>

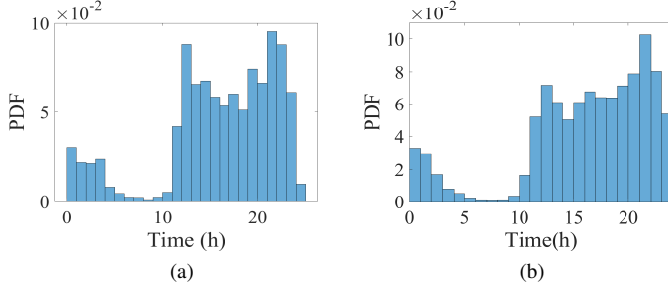


Fig. 3. Distribution of daily trips' end time (a) EVs (b) ICEVs

end of each trip ($\text{SOC}_k^{\text{arr}}$) and compare it to the start SOC of the next trip ($\text{SOC}_{k+1}^{\text{dep}}$) with k representing the trip index of the EV in the same day. If $\text{SOC}_{k+1}^{\text{dep}} > \text{SOC}_k^{\text{arr}}$, trip k would be a charging event starting at the end time of the same trip k . The CD can be calculated as the multiplication of the difference between SOC for the two consecutive trips or the required SOC (SOC^{req}) and the battery capacity of each EV (Cap_v):

$$\text{SOC}^{\text{req}} = \text{SOC}_{k+1}^{\text{dep}} - \text{SOC}_k^{\text{arr}} \quad (1)$$

$$\text{CD}_k = \begin{cases} \text{SOC}^{\text{req}} \times \text{Cap}_v & \text{if } \text{SOC}^{\text{req}} > 0 \\ 0 & \text{Otherwise} \end{cases} \quad (2)$$

The temporal behavior of CD also depends on the charging duration (ΔT), i.e., the amount of time required to receive the demanded energy (CD_k). This duration is directly proportional to the required CD and inversely proportional to the charging rate (α) and charging efficiency (η), which depend on the battery characteristics and the installed charger. This relation is presented in (3). We assumed that the demand (CD_k) will be imposed on the system at the end time of trip k lasting for a duration of ΔT_k .

$$\Delta T_k = \frac{\text{CD}_k}{\alpha \cdot \eta} \quad (3)$$

Additionally, the location of the charging event will be the destination of trip k , providing the spatial characteristics of the CD. Going through all the trips of EVs, we derived the charging location for each EV (see Fig. 4a) – locations are color-coded for different EVs. We observe more charging instances located in the central part of the city compared to the other regions. The study region can be divided into finite number of zones $\{z_i\}_{1 \leq i \leq n}$ covering different parts of the region, with n being the total number of zones, to categorize the spatial distribution of charging events. The system operator (SO) can divide the region based on its requirements and judgments to any number of zones with various shapes; To ensure each zone has enough number of charging records, here we have considered to have $n = 9$ charging zones as shown in Fig.4b, which will be used to estimate the spatial location of the CD.

From the power system prospective, the SO can use the calculated CD and the expected charging location for operational purposes, e.g., day-ahead generation dispatch, real time energy management, etc. Additionally, the system planner can use the predicted spatial-temporal CD for the future expansion of charging infrastructure and estimate the required charging

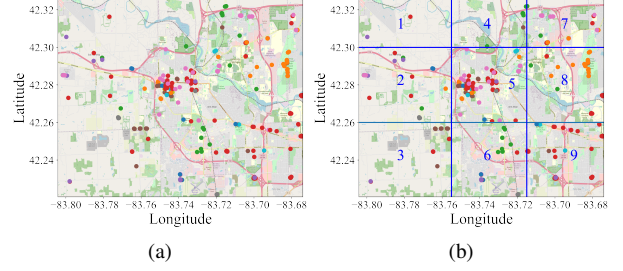


Fig. 4. (a) Spatial distribution of charging events for different EVs and (b) considered charging zones of the city

TABLE II
PROCESSED DATA EXAMPLE FOR THE FORECASTING MODELS

Vehicle ID	Trip No.	T^{str} (h)	T^{end} (h)	Origin location		Label	SOC^{dep} %	SOC^{req} %
				Latitude	Longitude			
371	1	13.44	13.75	42.277	-83.75	9	40.92	41.96
371	2	18.47	18.56	42.253	-83.674	10	45.69	0
371	3	18.96	19.06	42.256	-83.696	8	33.13	46.99
371	4	15.45	15.57	42.302	-83.704	10	64.67	0

station capacities at different locations.

V. METHODOLOGIES

In this section, we will develop forecasting models to estimate the spatiotemporal pattern of daily CD. In addition, we will prepare the input data and define our input features and targets.

A. Prepare Model Input Features

At the start of each trip, the known parameters are a) trip start time, b) origin location, and c) start SOC (SOC^{dep}). Our objective is to predict whether the EV will charge at the destination location; if yes, which zone and when this charging event will happen, and how much energy it will charge.

Predicting the choice of charging at the end of a trip and the charging zone can be modeled as a classification problem. We will label each charging event trip of the input data based on the number of the zone of the event $L = i$ ($1 \leq i \leq n$), defined in Section IV, and define a dummy zone $L = n + 1$ for the trips where no charging happens at the end of the trip. Table II shows how this labeling works on the example input data with $n = 9$. Trips 2 and 4 are not considered as charging event trips because $\text{SOC}^{\text{req}} < 0$ and trip 4 is the last trip of the day with no information of the next trip's SOC^{dep} in the next day (day 6). Therefore, the labels for these two trips are 10. Trips 1 and 3 are charging event trips with $\text{SOC}^{\text{req}} > 0$. The labels for these two trips are determined based on their destination locations, and they are in zones 9 and 8, respectively.

The temporal behavior of this CD depends on the end time and charging duration and can be determined based on the procedure presented in Section IV using (2) and (3).

In summary, the input features of our problem are vehicle ID and current trip's start time, origin location, and SOC^{dep} and we will use them to train the forecasting models.

B. Forecasting Models

The forecasting targets in our modeling are the label of the trip, trip end time, and SOC^{req} . Table III shows the input

TABLE III
INPUT FEATURES AND TARGETS OF THE EXAMPLE DATA

Vehicle ID	T^{str} (h)	Input features			Targets		
		SOC ^{dep} %	Origin location		Label	T^{end} (h)	SOC ^{req} %
371	13.44	40.92	42.277	-83.75	9	13.75	41.96
371	18.47	45.69	42.253	-83.674	10	18.56	0
371	18.96	33.13	42.256	-83.696	8	19.06	46.99
371	15.45	64.67	42.302	-83.704	10	15.57	0

TABLE IV
FORECASTING MODEL PARAMETERS

Target	KNN neighbors	DT tree depth	RF tree depth	ANN neurons	DANN	
					Layers	Neurons
Label	11	8	6	400	2	500,100
T^{end}	4	8	18	500	2	400,100
SOC ^{req}	10	4	5	400	3	900,500,100

features and the targets based on Table II as an example. Note that we calculate the CD only for trips with charging events, so we need to add charging labels as an input feature for forecasting the CD.

Five forecasting methods, namely K-nearest neighbor (KNN), decision tree (DT), random forest (RF), artificial neural networks (ANNs), and deep artificial neural networks (DANNs) were considered to predict each target. The considered methods have been widely used in machine learning applications and the detailed comparison on these methods are presented in [18]. We will train the models and determine their hyper parameters separately for each target with the defined input features. These parameters include the number of neighbors for the KNN method, tree depth for DT and RF methods, number of neurons for ANN, and number of neurons on each hidden layer for the DANN method. We investigated the performance of the models for a range of parameters by observing the accuracy of the classification for trip label prediction and the forecasting error for the trip end time and required SOC. The selected parameters and performance evaluation of the forecasting models are discussed in Section VI.

VI. RESULTS

A. Parameter Settings

Before feeding the input data to the forecasting models, we extract the trips made in days with charging event occurrence (1,062 trips) and split them into training sets and test sets – 25 % test set and 75% training sets. Scikit-learn library was used to train the KNN, DT, and RF models, and TensorFlow library were used to train the ANN based models. All the implementations were done on the Python software.

We trained the forecasting methods for a range of modeling parameters using the training sets and observed the performance of the methods on test set to select the best modeling parameters. Table IV summarizes the selected parameters for different forecasting methods. For the DANN method, the number of hidden layers more than the mentioned layers in Table IV resulted in less accuracy. Therefore, we limited the number of layers to 2 for CS zone (label) and trip end time prediction, and 3 layers for SOC^{req} prediction.

According to [19], the battery capacities of EVs studied in the VED data set is in the range of 20~25 KWh. Therefore,

TABLE V
PERFORMANCE OF FORECASTING MODELS ON THE TEST SET:
CLASSIFYING ACCURACY FOR LABEL PREDICTION AND RMSE VALUE
FOR T^{end} AND SOC^{req}

Target	KNN	DT	RF	ANN	DANN
Label (%)	63.91	63.53	73.97	65.73	65.78
T^{end} (h)	0.39	0.17	0.15	0.19	0.19
SOC ^{req} (%)	17.05	15.55	15.79	21.73	17.57

we consider the battery characteristics of Fiat500E, which is reported as one of the popular EVs in Alternative Fuels Data Center [20] and has a battery capacity of 24 KWh. We assume a charging rate of $\alpha = 6.6$ KW (i.e., level 2 charging) and the charging efficiency to be $\eta = 0.9$ [20] for CD demand calculations mentioned in (3).

B. Charging Demand Forecasting

After determining the parameters for each forecasting model, we compared their performance for predicting each target on the test data set (see Table V). The RF method provided the highest accuracy for charging zone label prediction and the least RMSE value for the trip end time and the DT method had the least RMSE value for predicting the required SOC. Even though ANN-based models have provided superior performance in other machine learning studies [3], [21], simpler models (KNN, DT, and RF) provided better results for our dataset. The low accuracy of label prediction stems from the small number of charging event trips (446 trips) compared to all of the trips made in days with charging events (1,062 trips) and a large number of classes/zones (10 classes).

We selected the best forecasting models for each target and predicted the spatiotemporal pattern of daily CD (see Figure 5). We considered two cases for forecasting the SOC^{req} 1) using the predicted labels as the input feature of the trained DT model and 2) using the actual labels of the trips. Charging start times were based on the predicted trip end times, and the resulting daily CDs were calculated using the procedure delineated in Section IV.

Comparing the estimated demands from case 1 and the test data (see Fig. 5a and 5c) shows that the developed classifier failed to detect the charging events in zone 1. This discrepancy is because of the less recorded charging events in this zone (see Fig. 4b). On the contrary, most of the charging events are predicted to occur at zone 5, which has more charging records in the input data, causing a significant spike in CD of this zone at $t = 11 \sim 12$. Moreover, the estimated CD for case 1 follows the temporal pattern of the CD during $t = 0 \sim 6$ but performs poorly in the afternoon (see Fig. 5a) because more charging events are predicted to be at zone 5 and most of the charging events in this zone happen in $t = 11 \sim 16$.

Passing the actual zones from the test data for forecasting the SOC^{req} (case 2) improved the temporal pattern in the afternoon and the nighttime (see Fig. 5b). The accurate charging zones have reduced the charging events in zone 5 and we no longer observe the high peak CD during $t = 11 \sim 12$ (compare Fig.5a and 5b). This increase in accuracy points out the importance of charging zone prediction in determining CD's temporal and spatial behavior.

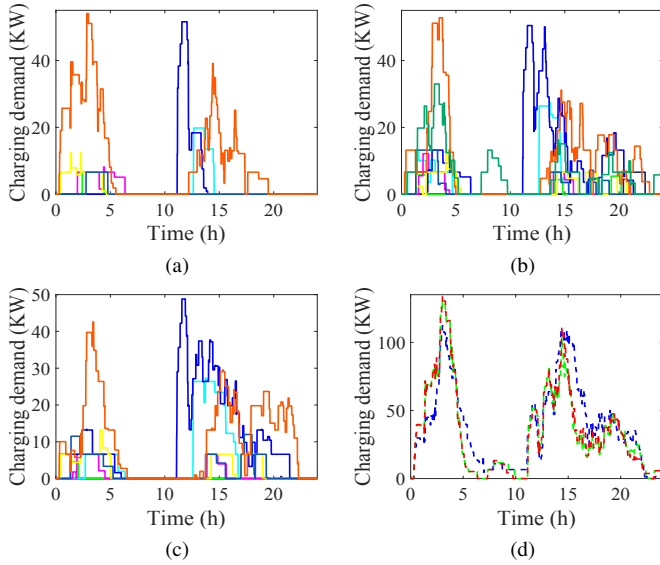


Fig. 5. Zonal CD for (a) case 1 (b) case 2 (c) test data, and (d) total CD; — zone 1, — zone 2, — zone 3, — zone 4, — zone 5, — zone 6, — zone 7, — zone 8, — zone 9; -.- Test data, -.- Estimated case 1, -.- Estimated case 2.

For comparing the temporal pattern of CD, we have derived the total daily CD (see Fig. 5d). The estimated CD after midnight until the morning ($t = 0 \sim 6$) follows the same pattern in both cases and resembles the actual CD derived from test data. However, in the afternoon, the prediction inaccuracy in charging zones resulted in inaccurate temporal estimates for case 1, especially after $t = 17$.

The SO and system planners can use the estimated spatio-temporal CD in different applications: 1) The predicted zonal CD in Fig. 5b can be used for day ahead generation dispatch and other operational planning purposes. For example, it is estimated that the CD at zone 8 would be high during the morning. Therefore, the SO would consider allotting sufficient energy generation in the day ahead planning of that zone. 2) The system planner can use the expected zonal CD for inferring user preferences and expanding the CS infrastructures. For example, the daily CD pattern shows higher CD at zones 5 and 8 compared to the other zones (see Fig. 5b), which can be good candidates for CS expansion.

VII. SUMMARY AND FUTURE EXTENSIONS

Estimating EVs' daily CD's spatial and temporal pattern is a vital factor in modeling uncertainties in power systems. CD pattern is closely related to the travel behavior of EVs. In this study, we use the VED, a high-resolution GPS data set of both EVs and conventional vehicles, to investigate the potential differences in the travel behavior of EVs and conventional vehicles and analyzed the real spatiotemporal pattern of CD. Our analyses showed that the travel behavior of EVs is similar to ICEVs in terms of trip start and end time, and trip distance. But EVs tend to have fewer daily trips compared to ICEVs.

After processing the GPS trajectories of EVs, we developed forecasting models to predict the spatiotemporal pattern of CD based on the known information at the starting point of the trips. The spatial pattern of CD was modeled as a classification

problem, where the charging event locations were grouped in different zones. The CD and its temporal pattern were estimated using a decision tree and random forest regressors with high accuracy.

The small scale of the input data limited the performance of the forecasting model, and we will examine the models on larger data sets as more data sets are becoming available for EVs. Future extension should also investigate the potential reasons of different predicting accuracy to better understand the applicability of machine learning algorithms. Another extension of this work is to develop a forecasting model to predict the daily CD based on the historical travel data rather than based on information at the starting point of each trip.

REFERENCES

- [1] H. Barbosa, M. Barthelemy *et al.*, "Human mobility: Models and applications," *Physics Reports*, vol. 734, pp. 1–74, 2018.
- [2] IEA, "Global EV outlook 2021, accelerating ambitions despite the pandemic," IEA: Paris, Tech. Rep., 2021. [Online]. Available: <https://www.iea.org/reports/global-ev-outlook-2021>
- [3] H. Jahangir, H. Tayarani *et al.*, "Charging demand of plug-in electric vehicles: Forecasting travel behavior based on a novel rough artificial neural network approach," *J. Clean. Prod.*, vol. 229, pp. 1029–1044, Aug. 2019.
- [4] M. Li, M. Lenzen, F. Keck *et al.*, "GIS-based probabilistic modeling of BEV charging load for australia," *IEEE Trans. Smart Grid*, vol. 10, no. 4, pp. 3525–3534, Apr. 2018.
- [5] S. Baghali, S. Hasan, and Z. Guo, "Analyzing the travel and charging behavior of electric vehicles-a data-driven approach," in *2021 IEEE Kansas Power and Energy Conference (KPEC)*. IEEE, 2021, pp. 1–5.
- [6] Z. Tian, Y. Wang, C. Tian *et al.*, "Understanding operational and charging patterns of electric vehicle taxis using gps records," in *17th International IEEE Conference on Intelligent Transportation Systems (ITSC)*. IEEE, Oct. 2014, pp. 2472–2479.
- [7] M. De Gennaro, E. Paffumi, H. Scholz, and G. Martini, "GIS-driven analysis of e-mobility in urban areas: An evaluation of the impact on the electric energy grid," *Appl. Energy*, vol. 124, pp. 94–116, Jul. 2014.
- [8] T. Yang, X. Xu, Q. Guo *et al.*, "EV charging behaviour analysis and modelling based on mobile crowdsensing data," *IET Gener. Transm.*, vol. 11, no. 7, pp. 1683–1691, Jan. 2017.
- [9] J. Fraile-Ardanuy, S. Castano-Solis, R. Álvaro-Hermana *et al.*, "Using mobility information to perform a feasibility study and the evaluation of spatio-temporal energy demanded by an electric taxi fleet," *Energy Convers. Manag.*, vol. 157, pp. 59–70, Feb. 2018.
- [10] R.-C. Leou, C.-L. Su, and C.-N. Lu, "Stochastic analyses of electric vehicle charging impacts on distribution network," *IEEE Trans. Smart Grid*, vol. 29, no. 3, pp. 1055–1063, Dec. 2013.
- [11] D. Tang and P. Wang, "Probabilistic modeling of nodal charging demand based on spatial-temporal dynamics of moving electric vehicles," *IEEE Trans. Smart Grid*, vol. 7, no. 2, pp. 627–636, Jun 2015.
- [12] M. B. Arias and S. Bae, "Electric vehicle charging demand forecasting model based on big data technologies," *Appl. Energy*, vol. 183, pp. 327–339, Dec. 2016.
- [13] S. Sun, Q. Yang, and W. Yan, "A novel markov-based temporal-SoC analysis for characterizing PEV charging demand," *IEEE Trans. Ind. Informat.*, vol. 14, no. 1, pp. 156–166, Jun 2017.
- [14] D. Panahi, S. Deilami *et al.*, "Forecasting plug-in electric vehicles load profile using artificial neural networks," in *2015 Australasian Universities Power Engineering Conference (AUPEC)*. IEEE, Sep. 2015, pp. 1–6.
- [15] A. Mansour-Saatloo, A. Moradzadeh *et al.*, "Machine learning based PEVs load extraction and analysis," *Electronics*, vol. 9, no. 7, p. 1150, July 2020.
- [16] G. Oh, D. J. Leblanc, and H. Peng, "Vehicle energy dataset (VED), a large-scale dataset for vehicle energy consumption research," *IEEE trans Intell Transp Syst*, 2020.
- [17] S. R. Khazeinyasab and J. Qi, "Resilience analysis and cascading failure modeling of power systems under extreme temperatures," *J. Mod. Power Syst. Clean Energy*, 2020.
- [18] S. D. Jadhav and H. Channe, "Comparative study of K-NN, naive bayes and decision tree classification techniques," *International Journal of Science and Research (IJSR)*, vol. 5, no. 1, pp. 1842–1845, 2016.
- [19] C. Prehofer and S. Mehmood, "Big data architectures for vehicle data analysis," in *2020 IEEE International Conference on Big Data (Big Data)*. IEEE, Dec. 2020, pp. 3404–3412.
- [20] U. S. D. of Energy. (2020) Alternative fuels data center. [Online]. Available: <https://afdc.energy.gov/>
- [21] H. Jahangir, H. Tayarani *et al.*, "A novel electricity price forecasting approach based on dimension reduction strategy and rough artificial neural networks," *IEEE Trans. Ind. Informat.*, vol. 16, no. 4, pp. 2369–2381, 2019.